2009 American Control Conference
Hyatt Regency Riverfront, St. Louis, MO, USA
June 10-12, 2009

Robust Nonlinear Control of a Hypersonic Aircraft in the Presence of Aerothermoelastic Effects

Z. D. Wilcox, W. MacKunis, S. Bhat, R. Lind, W. E. Dixon
Mechanical and Aerospace Engineering Department, University of Florida, Gainesville, FL 32611-6250
Email: {zibrus, mackunis, sanketh, ricklind, wdixon}@ufl.edu

Abstract— **Hypersonic flight conditions produce temperature variations that can alter the flight dynamics. A nonlinear temperature dependent, parameter varying state-space representation is proposed to capture the aerothermoelastic effects in a hypersonic vehicle. This model includes an uncertain parameter varying state matrix, an uncertain parameter varying non-square (column deficient) input matrix, and a nonlinear additive bounded disturbance. A Lyapunov-based continuous robust output feedback controller is developed that yields global exponential tracking of a reference model, despite the presence of disturbances that do not satisfy the linear-in-the parameters (LP) assumption.**

I. Introduction[1]

Design of guidance and control systems for airbreathing hypersonic vehicles (HSV) is a challenging task because the dynamics of the HSV are complex and highly coupled [1]. Moreover, temperature-induced stiffness variations impact the structural dynamics [2]. The structural dynamics, in turn, affect the aerodynamic properties. Vibration in the forward fuselage changes the apparent turn angle of the flow, which results in changes in the pressure distribution over the forebody of the aircraft. The resulting changes in the pressure distribution over the aircraft manifest themselves as thrust, lift, drag, and pitching moment perturbations [1]. To develop control laws for the longitudinal dynamics of a HSV capable of compensating for these structural and aerothermoelastic effects, surface temperature variations and structural dynamics must be considered.

Several results have examined the challenges associated with the dynamics and control of HSVs. A detailed analytical model of the longitudinal dynamics was undertaken by Chavez and Schmidt [3]. A slightly different approach to develop the model was undertaken by Bolender and Doman in [1] and [4], which was further developed by the same authors in [5] and [6]. Another model of the hypersonic vehicle was developed using piston theory [7]. Several results discuss various control strategies and sensor placement for the vehicle using the above models [8], [9]. In [10]–[12], HSV flight controllers are designed using genetic algorithms to search a design parameter space where the nonlinear longitudinal equations of motion contain uncertain parameters. The control designs in [10] and [11] utilize Monte Carlo simulations to estimate system robustness at each search iteration. The design in [12] uses fuzzy logic to control the attitude of the HSV about a single low end flight condition. While the approaches in [10]–[12] generate stabilizing controllers, the procedures are computationally demanding and require multiple evaluation simulations of the objective function. In [13], an adaptive gain-scheduled controller is designed. Using estimates of the scheduled parameters, a semi-optimal controller is developed to adaptively attain H_∞ control performance. The controller in [13] yields uniformly bounded stability due to the effects of approximation errors and algorithmic errors in the neural networks. Feedback linearization techniques are applied to the control-oriented HSV model derived in [14] to design a nonlinear controller. The model used in [14] is based on the HSV longitudinal dynamic model developed in [4]. The control design in [14] neglects variations in thrust lift parameters, altitude, and dynamic pressure. Two linear output feedback tracking control methods are presented in [8]. Sensor placement strategies are developed in the first controller to increase observability, and full state information is reconstructed and used with a state-feedback controller. A robust output feedback technique is developed for the second controller, which does not rely on state observation. In [8], the reference trajectories must be slow to avoid inducing oscillations in the inputs during the transient. There remains a need for a continuous controller, which is capable of achieving exponential tracking for a HSV dynamic model containing aerothermoelastic effects and unmodeled disturbances.

Aerothermoelasticity is the response of elastic structures to aerodynamic heating and loading. Aerothermoelastic effects cannot be ignored in hypersonic flight. The results in [2] illustrate that temperature effects can destabilize the HSV system. A loss of stiffness induced by aerodynamic heating was determined to potentially induce dynamic instability in supersonic/hypersonic flight speed regimes [15]. The result in [15] also illustrated that active control can be used to expand the flutter boundary and convert unstable limit cycle oscillations (LCO) to stable LCO. An active structural controller is developed in [16], which accounts for variations in the HSV structural properties resulting from aerothermoelastic effects. The control design in [16] models the structural dynamics using a LPV framework. As stated in [16], the benefits to using the LPV framework are two-fold: the dynamics can be represented as a single model, and controllers can be designed that have affine dependency on the operating

[1]This research is supported in part by NASA NNX07AC46A with program manager of Don Soloway.

parameters.

A nonlinear temperature-dependent parameter varying state-space representation is proposed in this paper to capture the aerothermoelastic effects in a hypersonic vehicle. This model includes an uncertain parameter varying state matrix, an uncertain parameter varying non-square (column deficient) input matrix, and a nonlinear additive bounded disturbance. A robust, continuous Lyapunov-based controller is developed that yields global exponential tracking of a reference model, despite the presence of disturbances that do not satisfy the linear-in-the parameters (LP) assumption.

II. HSV Model

A. Rigid Body & Elastic Dynamics

To incorporate structural dynamics and aerothermoelastic effects in the HSV dynamic model, an assumed modes model is considered for the longitudinal dynamics [5] as

$$\dot{V} = \frac{T\cos(\alpha) - D}{m} - g\sin(\theta - \alpha) \quad (1)$$

$$\dot{h} = V\sin(\theta - \alpha) \quad (2)$$

$$\dot{\alpha} = -\frac{L + T\sin(\alpha)}{mV} + Q + \frac{g}{V}\cos(\theta - \alpha) \quad (3)$$

$$\dot{\theta} = Q \quad (4)$$

$$\dot{Q} = \frac{M}{I_{yy}} \quad (5)$$

$$\ddot{\eta}_i = -2\zeta_i\omega_i\dot{\eta}_i - \omega_i^2\eta_i + N_i, \qquad i = 1,2,3. \quad (6)$$

In (1)-(6), $m \in \mathbb{R}$ denotes the vehicle mass, $I_{yy} \in \mathbb{R}$ is the moment of inertia, $g \in \mathbb{R}$ is the acceleration due to gravity, $T(t) \in \mathbb{R}$ denotes thrust, $D(t) \in \mathbb{R}$ denotes drag, $L(t) \in \mathbb{R}$ is lift, $V(t) \in \mathbb{R}$ denotes the forward velocity, and $M(t) \in \mathbb{R}$ is pitching moment about the body y-axis. In (6), $\zeta_i(t), \omega_i(t) \in \mathbb{R}$ are the damping factor and natural frequency of the i^{th} flexible mode, respectively, $\eta_i(t)$ $\forall i = 1,2,3$ denotes the i^{th} generalized structural mode displacement, and $N_i(t)$ $\forall i = 1,2,3$ denote generalized elastic forces. The terms $\theta(t), Q(t) \in \mathbb{R}$ are the pitch angle and pitch rate, respectively, and $\alpha(t) \in \mathbb{R}$ denotes the angle of attack. The equations that define the aerodynamic and generalized moments and forces are lengthy and are omitted for brevity. Details of the moments and forces are provided in [1]. Because of aerothermolelastic interactions, the temperature profile of the hypersonic vehicle will vary in time. As the temperature profile changes, the damping factors and natural frequencies of the flexible modes will change.

B. Temperature Profile Model

The effects of temperature variation on the flight dynamics of a HSV need to be analyzed and understood to develop an effective control law. The temperature variations have an impact on the structural dynamics as it affects the mode shapes and natural frequencies, and hence, the flight dynamics. The natural frequencies of a continuous beam are a function of the mass distribution of the beam and the stiffness. In turn, the stiffness is a function of Young's Modulus (E) and admissible mode functions. Hence, by modeling Young's Modulus as a function of temperature, the effect of temperature on flight dynamics can be captured.

TABLE I

Natural frequencies for the 5 Linear Temperature Profiles.

Mode	1	2	3	4	5	Reduction
1	23.0	23.5	23.9	24.3	24.7	6.96 %
2	49.9	50.9	51.8	52.6	53.5	6.85 %
3	98.9	101.0	102.7	104.4	106.2	6.88 %

Different temperature gradients along the fuselage are introduced into the model. The subsequent analysis is restricted to decreasing gradients from the nose to the tail as it is expected that the nose will always be the hottest part of the structure. The material of the fuselage below the thermal protection system is assumed to be Titanium [6], [17]. Fig. 1 shows the fifteen temperature profiles introduced into the model.

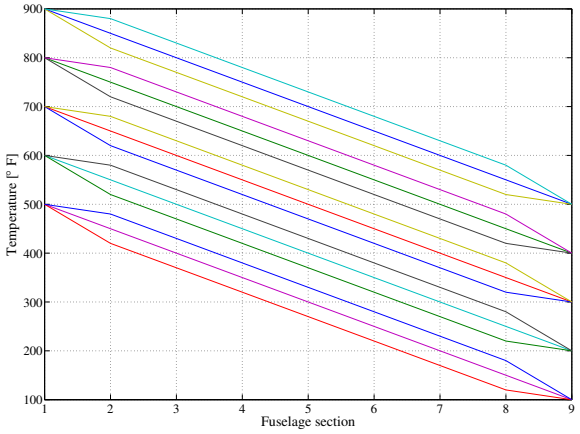

Fig. 1. HSV surface temperature profiles varying between $T_{nose} = 900^0F$, $T_{tail} = 500^0F$ and $T_{nose} = 500^0F$, $T_{tail} = 100^0F$.

Table I shows the variation in the natural frequencies for the linear temperature profiles. For all three natural modes, Table I shows that the natural frequency for the first temperature profile is almost 7% lower than that of the fifth temperature profile. Fig. 2 shows the mode shapes for a single temperature profile. The asymmetric shape of the modes shown in Fig. 2 is due to the variations in Young's Modulus resulting from the fact that each of the 9 fuselage sections (see Fig. 1) has a different temperature.

C. Control Model

Based on [16], the HSV dynamics can be modeled as a combination of linear-parameter-varying (LPV) state matrices and nonlinearities arising from unmodeled effects as

$$\dot{x} = A(\rho(t))x + B(\rho(t))u + f(t) \quad (7)$$

$$y = Cx. \quad (8)$$

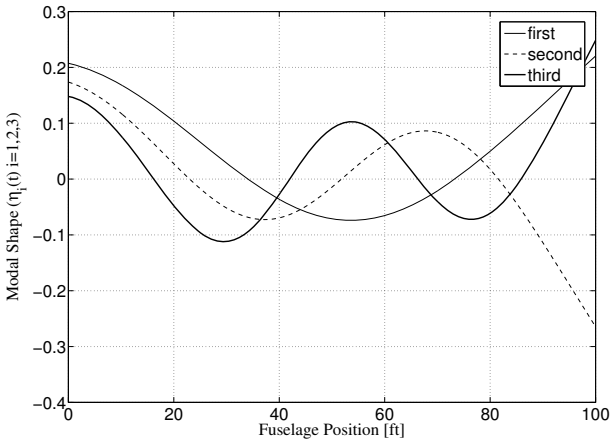

Fig. 2. Mode shapes for the hypersonic vehicle.

In (7) and (8), the state vector $x(t) \in \mathbb{R}^{11}$ is composed of 5 flight and 6 structural dynamic states including both modal velocity $\dot{\eta}_i(t)$ and displacement $\eta_i(t)$. Also in (7), $A(\rho(t)) \in \mathbb{R}^{11\times 11}$ denotes a linear parameter varying state matrix, $B(\rho(t)) \in \mathbb{R}^{11\times 3}$ denotes a column deficient, linear parameter varying input matrix, $C \in \mathbb{R}^{3\times 11}$ denotes a known output matrix, $u(t) \in \mathbb{R}^3$ denotes a vector of control inputs, $\rho(t)$ represents the unknown time-dependent temperature profile of the aircraft, and $f(t) \in \mathbb{R}^{11}$ represents a time-dependent unknown, nonlinear disturbance.

The matrices $A(\rho(t))$ and $B(\rho(t))$, have the standard linear parameter-varying form [16]

$$A(\rho,t) = A_0 + \sum_{i=1}^{s} w_i(\rho(t)) A_i \quad (9)$$

$$B(\rho,t) = B_0 + \sum_{i=1}^{s} v_i(\rho(t)) B_i \quad (10)$$

where $A_0 \in \mathbb{R}^{11\times 11}$ and $B_0 \in \mathbb{R}^{11\times 3}$ represent known nominal matrices with unknown variations $w_i(\rho(t)) A_i$ and $v_i(\rho(t)) B_i$ for $i = 1, 2, ..., s$, where $A_i \in R^{11\times 11}$ and $B_i \in R^{11\times 3}$ are time-invariant matrices, and $w_i(\rho(t)), v_i(\rho(t)) \in \mathbb{R}$ are parameter-dependent weighting terms. Knowledge of the nominal matrix B_0 will be exploited in the subsequent control design.

The state, output, and input vectors are given explicitly as

$$\begin{aligned} x &= \begin{bmatrix} V & \alpha & Q & h & \theta & \eta_1 & \dot{\eta}_1 & \eta_2 & \dot{\eta}_2 & \eta_3 & \dot{\eta}_3 \end{bmatrix}^T \\ y &= \begin{bmatrix} V & \alpha & Q \end{bmatrix}^T \\ u &= \begin{bmatrix} \delta_e & \delta_c & A_d & \phi_f \end{bmatrix}^T \end{aligned} \quad (11)$$

where $\delta_e(t)$ and $\delta_c(t)$ denote the elevator and canard deflection angles, respectively, $A_d(t)$ is the diffuser nozzle area ratio, $\phi_f(t)$ is the fuel mixture ratio, and the output and state variables are introduced in (1)-(5).

Remark 1: The control inputs being used are $\delta_e(t)$, $\delta_c(t)$, and $A_d(t)$. The fuel mixture ratio $\phi_f(t)$ is left at its operational trim condition without loss of generality.

To facilitate the subsequent control design, a reference model is given as

$$\dot{x}_m = A_m x_m + B_m \delta \quad (12)$$

$$y_m = C x_m \quad (13)$$

where $A_m \in \mathbb{R}^{11\times 11}$ and $B_m \in \mathbb{R}^{11\times 3}$ denote the state and input matrices, respectively, where A_m is Hurwitz, $\delta(t) \in \mathbb{R}^3$ is a vector of reference inputs, $y_m(t) \in \mathbb{R}^3$ are the reference outputs, and C was defined in (8). The design is intended to exhibit favorable transient response characteristics and to achieve zero steady-state error.

Assumption 1: The nonlinear disturbance $f(t)$ and its first two time derivatives are assumed to exist and be bounded by known constants.

Assumption 2: The matrices $A(\rho(t))$ and $B(\rho(t))$ and their time derivatives satisfy the following inequalities:

$$\begin{aligned} \|A(\rho(t))\|_{i\infty} \le \zeta_A \qquad \|B(\rho(t))\|_{i\infty} \le \zeta_B \\ \left\|\dot{A}(\rho(t))\right\|_{i\infty} \le \zeta_{Ad} \qquad \left\|\dot{B}(\rho(t))\right\|_{i\infty} \le \zeta_{Bd} \end{aligned} \quad (14)$$

where $\zeta_A, \zeta_B, \zeta_{Ad}, \zeta_{Bd} \in \mathbb{R}^+$ are known bounding constants, and $\|\cdot\|_{i\infty}$ denotes the induced infinity norm of a matrix.

III. Control Development

A. Control Objective

The control objective is to ensure that the output $y(t)$ tracks the time-varying output generated from the reference model in (12) and (13). To quantify the control objective, an output tracking error, denoted by $e(t) \in \mathbb{R}^3$, is defined as

$$e \triangleq y - y_m = C(x - x_m). \quad (15)$$

To facilitate the subsequent analysis, a filtered tracking error [18], denoted by $r(t) \in \mathbb{R}^3$, is defined as

$$r \triangleq \dot{e} + \gamma e \quad (16)$$

where $\gamma \in \mathbb{R}$ is a positive, constant control gain. To facilitate the subsequent robust control development, the state vector $x(t)$ is expressed as

$$x(t) = \underline{x}(t) + x_u(t) \quad (17)$$

where $\underline{x}(t) \in \mathbb{R}^{11}$ contains the 3 output states, and $x_u(t) \in \mathbb{R}^{11}$ contains the remaining 8 states. Likewise, the reference states $x_m(t)$ can also be separated as in (17).

Assumption 3: The states contained in $x_u(t)$ in (17) and the corresponding time derivatives can be further separated as

$$\begin{aligned} x_u(t) &= x_{\rho u}(t) + x_{\zeta u}(t) \\ \dot{x}_u(t) &= \dot{x}_{\rho u}(t) + \dot{x}_{\zeta u}(t) \end{aligned} \quad (18)$$

where $x_{\rho u}(t), \dot{x}_{\rho u}(t), x_{\zeta u}(t), \dot{x}_{\zeta u}(t) \in \mathbb{R}^{11}$ are upper bounded as

$$\begin{aligned} \|x_{\rho u}(t)\| &\le c_1 \|z\| \qquad \|x_{\zeta u}(t)\| \le \zeta_{xu} \\ \|\dot{x}_{\rho u}(t)\| &\le c_2 \|z\| \qquad \|\dot{x}_{\zeta u}(t)\| \le \zeta_{\dot{x}u} \end{aligned} \quad (19)$$

where $z(t) \in \mathbb{R}^6$ is defined as

$$z \triangleq \begin{bmatrix} e^T & r^T \end{bmatrix}^T \tag{20}$$

and $c_1, c_2, \zeta_{xu}, \zeta_{\dot{x}u} \in \mathbb{R}$ are known non-negative bounding constants (i.e., the constants could be zero for different classes of systems).

B. Open-Loop Error System

The open-loop tracking error dynamics can be developed by taking the time derivative of (16) and using the expressions in (7)-(13) to obtain

$$\dot{r} = \tilde{N} + N_d + C\dot{B}u + CB\dot{u} - e. \tag{21}$$

The auxiliary functions $\tilde{N}\left(x, \dot{x}, e, x_m, \dot{x}_m, t\right) \in \mathbb{R}^3$ and $N_d\left(x_m, \dot{x}_m, \delta, \dot{\delta}, t\right) \in \mathbb{R}^3$ in (21) are defined as

$$\begin{aligned} \tilde{N} \triangleq\ & CA\left(\underline{\dot{x}} - \underline{\dot{x}}_m\right) + C\dot{A}\left(\underline{x} - \underline{x}_m\right) \\ & + CA\dot{x}_{\rho u} + C\dot{A}x_{\rho u} + \gamma\dot{e} + e \end{aligned} \tag{22}$$

and

$$\begin{aligned} N_d \triangleq\ & C\dot{f}(t) + CA\dot{x}_{\zeta u} + C\dot{A}x_{\zeta u} \\ & + CA\underline{\dot{x}}_m + C\dot{A}\underline{x}_m - CA_m\dot{x}_m - CB_m\dot{\delta}. \end{aligned} \tag{23}$$

Motivation for the selective grouping of the terms in (22) and (23) is derived from the fact that the following inequalities can be developed [19], [20]:

$$\left\|\tilde{N}\right\| \leq \rho_0 \|z\| \qquad \|N_d\| \leq \zeta_{N_d}, \tag{24}$$

where $\rho_0, \zeta_{N_d} \in \mathbb{R}^+$ are known bounding constants.

C. Closed-Loop Error System

Based on the expression in (21) and the subsequent stability analysis, the control input is designed as

$$\begin{aligned} u =\ & -(CB_0)^{-1}\left[\left(k_s + I_{3\times 3}\right)e(t) - \left(k_s + I_{3\times 3}\right)e(0)\right] \\ & - (CB_0)^{-1}\int_0^t \left(k_u \|u(\sigma)\| sgn(r(\sigma)) \right. \\ & \left. + \left(k_s + I_{3\times 3}\right)\gamma e(\sigma) + k_\gamma sgn(r(\sigma))\right) d\sigma \end{aligned} \tag{25}$$

where $k_u, k_s, k_\gamma \in \mathbb{R}^{3\times 3}$ denote positive definite, diagonal constant control gain matrices, $B_0 \in \mathbb{R}^{11\times 3}$ is introduced in (10), $sgn(\cdot)$ denotes the standard signum function where the function is applied to each element of the vector argument, and $I_{q\times q}$ denotes a $q \times q$ identity matrix. A possible deficit of this control design is that it requires measurement of the sign of the acceleration-dependent term $r(t)$. However, in the context of flight control, it is commonly assumed that acceleration measurements are available [21]–[23]. For example, in [24], lateral acceleration measurements are provided by an Inertial Measurement Unit (IMU), and a high-gravity SOI-MEMS accelerometer is used in [25] to measure flight acceleration.

After substituting the time derivative of (25) into (21), the error dynamics can be expressed as

$$\begin{aligned} \dot{r} =\ & \tilde{N} + N_d - \tilde{\Omega}k_u \|u(t)\| sgn(r(t)) \\ & + C\dot{B}u - \tilde{\Omega}\left(k_s + I_{3\times 3}\right)r(t) \\ & - \tilde{\Omega}k_\gamma sgn(r(t)) - e \end{aligned} \tag{26}$$

where the auxiliary matrix $\tilde{\Omega}(\rho(t)) \in \mathbb{R}^{3\times 3}$ is defined as

$$\tilde{\Omega} \triangleq CB(CB_0)^{-1} \tag{27}$$

where $\tilde{\Omega}(\rho(t))$ can be separated into diagonal (i.e., $\Lambda(\rho(t)) \in \mathbb{R}^{3\times 3}$) and off-diagonal (i.e., $\Delta(\rho(t)) \in \mathbb{R}^{3\times 3}$) components as

$$\tilde{\Omega} = \Lambda + \Delta. \tag{28}$$

Assumption 4: The subsequent development is based on the assumption that the uncertain matrix $\tilde{\Omega}(\rho(t))$ is diagonally dominant in the sense that

$$\lambda_{\min}(\Lambda) - \|\Delta\|_{i\infty} > \varepsilon \tag{29}$$

where $\varepsilon \in \mathbb{R}^+$ is a known constant. Preliminary results show this assumption is mild in the sense that (29) is satisfied for a wide range of $B(\rho(t)) \neq B_0$.

IV. Stability Analysis

Theorem 1: The controller given in (25) ensures that the output tracking error is regulated in the sense that

$$\|e(t)\| \leq \|z(0)\| \exp(-\lambda_1 t) \qquad \forall t \in [0, \infty) \tag{30}$$

where $\lambda_1 \in \mathbb{R}^+$ is a constant, provided the control gains k_u, k_s, and k_γ introduced in (25) are selected according to the following sufficient conditions:

$$\lambda_{\min}(k_u) \geq \frac{\zeta_{Bd}}{\varepsilon} \qquad \lambda_{\min}(k_s) > \frac{\rho_0^2}{4\varepsilon \min\{\gamma, \varepsilon\}} \tag{31}$$

$$\lambda_{\min}(k_\gamma) > \frac{\zeta_{N_d}}{\varepsilon} \tag{32}$$

where ρ_0 and ζ_{N_d} are introduced in (24), ε is introduced in (29), ζ_{Bd} is introduced in (14), and $\lambda_{\min}(\cdot)$ denotes the minimum eigenvalue of the argument.

Proof: Let $V_L(z,t) : \mathbb{R}^6 \times [0,\infty) \to \mathbb{R}$ be a continuously differentiable, positive definite function defined as

$$V_L(z,t) \triangleq \frac{1}{2}e^T e + \frac{1}{2}r^T r \tag{33}$$

where $e(t)$ and $r(t)$ are defined in (15) and (16), respectively. After taking the time derivative of (33) and utilizing (16), (26), and (28), $\dot{V}_L(z,t)$ can be expressed as

$$\begin{aligned} \dot{V}_L(z,t) =\ & -\gamma e^T e + r^T\tilde{N} + r^T C\dot{B}u \\ & - r^T\Lambda\left(k_s + I_{3\times 3}\right)r - r^T\Delta\left(k_s + I_{3\times 3}\right)r \\ & - r^T\Lambda\|u(t)\| k_u sgn(r) \\ & - r^T\Delta\|u(t)\| k_u sgn(r) \\ & - r^T\Lambda k_\gamma sgn(r) - r^T\Delta k_\gamma sgn(r) + r^T N_d. \end{aligned} \tag{34}$$

After utilizing (14), (24), and (29), $\dot{V}_L(z,t)$ can be upper bounded as

$$\begin{aligned} \dot{V}_L(z,t) \leq\ & -\gamma\|e\|^2 - \varepsilon\|r\|^2 - \left[\varepsilon\lambda_{\min}(k_\gamma) - \zeta_{N_d}\right]\|r\| \\ & - \left[\varepsilon\lambda_{\min}(k_u) - \zeta_{Bd}\right]\|r\|\|u\| \\ & + \rho_0\|r\|\|z\| - \varepsilon\lambda_{\min}(k_s)\|r\|^2. \end{aligned} \tag{35}$$

If k_u and k_γ satisfy the sufficient gain conditions in (31) and (32), the bracketed terms in (35) are positive, and $\dot{V}_L(z,t)$

can be upper bounded using the squares of the components of $z(t)$ as:

$$\dot{V}_L(z,t) \leq -\gamma \|e\|^2 - \varepsilon \|r\|^2 - \left[\varepsilon \lambda_{\min}(k_s) \|r\|^2 - \rho_0 \|r\| \|z\|\right]. \quad (36)$$

Completing the squares for the bracketed terms in (36) yields

$$\dot{V}_L(z,t) \leq -\left(\min\{\gamma, \varepsilon\} - \frac{\rho_0^2}{4\varepsilon \lambda_{\min}(k_s)}\right) \|z\|^2. \quad (37)$$

The inequality in (37) can be used to show that $V_L(t) \in \mathcal{L}_\infty$; hence $e(t), r(t) \in \mathcal{L}_\infty$. Given that $e(t), r(t) \in \mathcal{L}_\infty$, standard linear analysis methods can be used to prove that $\dot{e}(t) \in \mathcal{L}_\infty$ from (16). Since $e(t), \dot{e}(t) \in \mathcal{L}_\infty$, the assumption that $y_m(t), \dot{y}_m(t) \in \mathcal{L}_\infty$ can be used along with (15) to prove that $y(t), \dot{y}(t) \in \mathcal{L}_\infty$. Given that $y(t), \dot{y}(t), e(t), r(t) \in \mathcal{L}_\infty$, the vector $\underline{x}(t) \in \mathcal{L}_\infty$, the time derivative $\dot{\underline{x}}(t) \in \mathcal{L}_\infty$, and (17)-(19) can be used to show that $x(t), \dot{x}(t) \in \mathcal{L}_\infty$. Given that $x(t), \dot{x}(t) \in \mathcal{L}_\infty$, Assumptions 1 and 2 can be utilized along with (7) to show that $u(t) \in \mathcal{L}_\infty$.

The definition for $V_L(z,t)$ in (33) can be used along with inequality (37) to show that $V_L(z,t)$ can be upper bounded as

$$\dot{V}_L(z,t) \leq -\lambda_2 V_L(z,t) \quad (38)$$

where $\lambda_2 \in \mathbb{R}^+$ is a constant, provided the sufficient condition in (31) is satisfied. The differential inequality in (38) can be solved as

$$V_L(z,t) \leq V_L(z(0),0) \exp(-\lambda_2 t). \quad (39)$$

Hence, (20), (33), and (39) can be used to bound $z(t)$ as

$$\|z(t)\| \leq \|z(0)\| \exp\left(-\frac{\lambda_2}{2} t\right) \qquad \forall t \in [0, \infty). \quad (40)$$

Based on the definition of $z(t)$, (40) can be used to show that

$$\|e(t)\| \leq \|z(0)\| \exp\left(-\frac{\lambda_2}{2} t\right) \qquad \forall t \in [0, \infty). \quad (41)$$

■

V. Conclusion

A robust HSV tracking controller is presented, which achieves global exponential tracking control of a model reference system where the plant dynamics contain state-varying parametric uncertainty, aerothermoelastic effects, and a bounded non-LP disturbance. This result represents the first ever application of a continuous, robust model reference control strategy for a HSV system with additive, non-LP disturbances and aerothermoelastic effects, where the control input is multiplied by an uncertain, column deficient, parameter-varying matrix. A Lyapunov-based stability analysis is provided to verify the theoretical result and indicates the proposed controller is robust to sensor noise, exogenous perturbations, parametric uncertainty, and plant nonlinearities, while simultaneously exhibiting the capability to emulate a reference model.

References

[1] M. A. Bolender and D. B. Doman, "Nonlinear longitudinal dynamical model of an air-breathing hypersonic vehicle," *Journal of Spacecraft and Rockets*, vol. 44, no. 2, pp. 374–387, Apr. 2007.

[2] J. Heeg, T. A. Zeiler, A. S. Pototzky, and C. V. Spain, "Aerothermoelastic analysis of a NASP demonstrator model," AIAA Paper 93-1366, Apr. 1993.

[3] F. Chavez and D. Schmidt, "Analytical aeropropulsive/aeroelastic hypersonic-vehicle model with dynamic analysis," *Journal of Guidance, Control and Dynamics*, vol. 17, no. 6, pp. 1308–1319, 1994.

[4] M. Bolender and D. Doman, "A non-linear model for the longitudinal dynamics of a hypersonic air-breathing vehicle," in *AIAA Guidance, Navigation and Control Conf.*, San Francisco, CA, Aug. 2005.

[5] T. Williams, M. A. Bolender, D. B. Doman, and O. Morataya, "An aerothermal flexible mode analysis of a hypersonic vehicle," in *AIAA Paper 2006-6647*, Aug. 2006.

[6] A. J. Culler, T. Williams, and M. A. Bolender, "Aerothermal modeling and dynamic analysis of a hypersonic vehicle," in *AIAA Atmospheric Flight Mechanics Conf.*, Hilton Head, SC, Aug. 2007.

[7] M. Oppenheimer, T. Skijins, M. Bolender, and D. Doman, "A flexible hypersonic vehicle model developed with piston theory," in *AIAA Atmospheric Flight Mechanics Conf.*, Hilton Head, SC, Aug. 2007.

[8] P. Jankovsky, D. O. Sigthorsson, A. Serrani, and S. Yurkovich, "Output feedback control and sensor placement for a hypersonic vehicle model," in *AIAA Guidance, Navigation, and Control Conf.*, Hilton Head, SC, Aug. 2007.

[9] L. Fiorentini, A. Serrani, M. A. Bolender, and D. B. Doman, "Nonlinear robust/adaptive controller design for an air-breathing hypersonic vehicle model," in *AIAA Guidance, Navigation, and Control Conf.*, Hilton Head, SC, Aug. 2007.

[10] C. I. Marrison and R. F. Stengel, "Design of robust control systems for a hypersonic aircraft," *Journal of Guidance, Control, and Dynamics*, vol. 21, no. 1, pp. 58–63, Jan.-Feb. 1998.

[11] Q. Wang and R. F. Stengel, "Robust nonlinear control of a hypersonic aircraft," *Journal of Guidance, Control, and Dynamics*, vol. 23, no. 4, pp. 577–585, Aug. 2000.

[12] K. J. Austin and P. A. Jacobs, "Application of genetic algorithms to hypersonic flight control," in *IFSA World Congress and 20th NAFIPS International Conference*, Vancouver, British Columbia, Canada, July 2001, pp. 2428–2433.

[13] M. Yoshihiko, "Adaptive gain-scheduled H-infinity control of linear parameter-varying systems with nonlinear components," in *American Control Conf.*, Denver, CO, June 2003, pp. 208–213.

[14] J. T. Parker, A. Serrani, S. Yurkovich, M. A. Bolender, and D. B. Doman, "Control-oriented modeling of an air-breathing hypersonic vehicle," in *Journal of Guidance, Control, and Dynamics*, 2007.

[15] L. K. Abbasa, C. Qian, P. Marzocca, G. Zafer, and A. Mostafa, "Active aerothermoelastic control of hypersonic double-wedge lifting surface," *Chinese Journal of Aeronautics*, vol. 21, pp. 8–18, 2008.

[16] R. Lind, "Linear parameter-varying modeling and control of structural dynamics with aerothermoelastic effects," *Journal of Guidance, Control, and Dynamics*, vol. 25, no. 4, pp. 733–739, July-Aug. 2002.

[17] M. Bolender and D. Doman, "Modeling unsteady heating effects on the strucutral dynamics of a hypersonic vehicle," in *AIAA Atmospheric Flight Mechanics Conf.*, Keystone, CO, Aug. 2006.

[18] F. L. Lewis, C. T. Abdallah, and D. M. Dawson, *Control of Robot Manipulators*. New York, NY: MacMillan, 1993.

[19] P. M. Patre, W. MacKunis, C. Makkar, and W. E. Dixon, "Asymptotic tracking for systems with structured and unstructured uncertainties," *IEEE Transactions on Control Systems Technology*, vol. 16, no. 2, pp. 373–379, 2008.

[20] B. Xian, D. M. Dawson, M. S. de Queiroz, and J. Chen, "A continuous asymptotic tracking control strategy for uncertain nonlinear systems," *IEEE Transactions on Automatic Control*, vol. 49, no. 7, pp. 1206–1211, July 2004.

[21] T. Wagner and J. Valasek, "Digital autoland control laws using quantitative feedback theory and direct digital design," *Journal of Guidance, Control and Dynamics*, vol. 30, no. 5, pp. 1399–1413, Sept. 2007.

[22] M. Bodson, "Multivariable adaptive algorithms for reconfigurable flight control," in *Proc. of Conf. on Decision and control*, Lake Buena Vista, FL, Dec. 1994, pp. 12.E.5–121–10.

[23] B. J. Bacon, A. J. Ostroff, and S. M. Joshi, "Reconfigurable NDI controller using inertial sensor failure detection & isolation," *IEEE Transactions on Aerospace and Electronic Systems*, vol. 37, no. 4, pp. 1373–1383, Oct. 2001.

[24] V. Janardhan, D. Schmitz, and S. N. Balakrishnan, "Development and implementation of new nonlinear control concepts for a UA," in *Proc. of Digital Avionics Systems Conf.*, Salt Lake City, UT, Oct. 2004, pp. 12.E.5–121–10.

[25] B. S. Davis, T. Denison, and J. Kaung, "A monolithic high-g SOI-MEMS accelerometer for measuring projectile launch and flight accelerations," in *Proc. of Conf. on Sensors*, Vienna, Austria, Oct. 2004, pp. 296–299.